JOURNAL OF SOLID STATE CHEMISTRY **62**, 172–176 (1986)

Neutron Powder Diffraction Study of Tetragonal Crystal Structures of Cerium–Neodymium Dicarbides

D. W. JONES,* I. J. McCOLM,† R. STEADMAN,‡ AND J. YERKESS*

*Schools of *Chemistry, †Industrial Technology, and ‡Materials Science, University of Bradford, Bradford, West Yorkshire, BD7 1DP, Great Britain*

Received May 8, 1985; in revised form August 20, 1985

The three ternary cerium–neodymium dicarbides $Ce_xNd_{1-x}C_2$ ($x = 0.25, 0.50, 0.75$) and the two binary dicarbides CeC_2 and NdC_2 have been prepared and their room temperature crystal structures examined by neutron powder diffraction by the Rietveld profile analysis method. The five compounds are isostructural, with tetragonal unit cell dimensions changing monotonically over the range $a = 3.881(2)$, $c = 6.487(3)$ Å to $a = 3.827(2)$, $c = 6.407(2)$ Å and they contain discrete acetylenic C–C groups with carbon–carbon bond lengths close to 1.29(1) Å. © 1986 Academic Press, Inc.

1. Introduction

The structure, bonding, and phase transitions of saltlike binary and ternary lanthanide carbides continue to be of interest in view of potential technological applications of their mechanical and electrical properties. Crystallographic variations of symmetry with composition tend to be more marked for ternary dicarbides with elements relatively widely separated in atomic number. Among the lower atomic number rare earth dicarbides, there may be a greater tendency for disordered structures.

For the extreme members of the Ce/Nd series, CeC_2 and NdC_2, the transformations from the high-temperature cubic form to the lower-temperature body-centered tetragonal form occur at 1360 and 1420 K (*1*), respectively (melting points are ≥ 2500 K). While the ternary carbides of intermediate composition will have lower transformation temperatures, they will all be expected to be tetragonal at room temperature. The ionic radii of Ce and Nd differ rather more than those of Y and Ho (*5*) but they are insufficiently different for the cubic phase to exist at room temperature. Both X-ray (*2*) and neutron diffraction (*3*) measurements confirm that CeC_2 and NdC_2 crystallize in the tetragonal space group D_{4h}–*I4/mmm* but they undergo antiferromagnetic transitions at 33 and 29 K.

For location of low atomic number elements, such as carbon, in the presence of high atomic number elements, such as the rare earths, neutron diffraction is preferable to X-ray diffraction. While least-squares refinement of a small number of individual integrated Bragg reflections may be satisfactory for cubic structures, with lower symmetries the Rietveld neutron powder-profile refinement procedure (*4*) is advantageous.

In continuation of our study of the struc-

0022-4596/86 $3.00

tures of ternary rare earth and other heavy metal dicarbides (*5*), we present here powder neutron diffraction studies of the room temperature crystal structures of the dicarbides $Ce_xNd_{1-x}C_2$ over the range $x = 0–1$.

2. Experimental Details

2.1 Sample Preparation

Preparation of the five dicarbides was analogous to that of the yttrium–holmium dicarbides described previously (*5*), i.e., each involved the addition of products from a batch of small-scale runs by direct high-temperature synthesis from stoichiometric quantities of the constituent elements in a small argon arc furnace. The lanthanide metals (minimum purity 99.9%, supplied as arc-melted rods by Rare-Earth Products, Ltd.) and the Specpure rods of graphite (in slight excess, over stoichiometry) were used as coarse lumps to minimize losses in the arc flame (*1*). Phase purity was checked by optical microscopy and X-ray powder photographs and by absence of lines due to graphite on the neutron diffraction powder patterns.

2.2 Collection of Neutron–Diffraction Data

The neutron diffraction pattern of each sample, contained in a thin-walled 5-mm-diameter cylindrical vanadium can, was recorded at room temperature on the VANESSA multi-detector powder diffractometer at the HERALD low-flux reactor at AWRE, Aldermaston, with slit angles $\alpha_1 = 112$ min, $\alpha_2 = 25$ min, and $\alpha_3 = 25$ min. The neutron wavelength (determined from a powder diffraction pattern on annealed nickel powder) was 1.100 Å, and the step increment was 0.1° over a 2θ range from −10° to +110°. Since the VANESSA diffractometer has eight detectors radially disposed at 15° intervals around the specimen axis, a 15° scan is sufficient to cover the complete 2θ range. With a counting time of about 14 min per point, the complete diffraction pattern was obtained in about 35 hr. The counts were normalized manually to correct for the different counter efficiencies.

For $Ce_{0.5}Nd_{0.5}C_2$, a second diffraction pattern was recorded after the material had been annealed for about 50 hr at 1370 K. Since this pattern did not differ perceptibly from that from the unannealed material, it was not examined further.

2.3 Structure Refinement

The qualitatively similar diffraction patterns for all five materials were taken to confirm the calcium dicarbide structure. The absence of superlattice lines in the ternary compounds was interpreted as indicating random occupation of the metal atom sites by the two metal species in these structures. The starting point for the refinement of all five structures was, therefore, the body-centered tetragonal structure (space group *I4/mmm*) established by Spedding *et al.* (*2*) by X-ray powder diffraction for CeC_2 and NdC_2 and confirmed by Atoji (*3*) by refinement of neutron-diffraction powder-peak intensities.

The profile refinements (*4*) followed the same least-squares minimization procedure as described previously (*5*), with 13 crystal-structural and instrumental variables, and with the anisotropic thermal parameters subject to the constraints (*6*) $B_{11} = B_{22}$ and $B_{12} = B_{13} = B_{23} = 0$ for both metal and carbon atoms. Details of initial values for the variables are as follows:

(1) Unit cell parameters (a and c) for CeC_2 and NdC_2 were taken from Spedding *et al.* (*2*) with linearly interpolated values for the mixed cerium/neodymium compositions.

(2) $B_{11} = B_{33} = 0.5$ Å^2 for both metal and carbon atoms.

(3) The z parameter for the carbon atom was taken from Atoji (*3*) for CeC_2 and

NdC_2, with linearly interpolated values for the mixed cerium/neodymium compositions.

(4) The initial value of the scale factor was obtained from several preliminary cycles of least-squares refinement in which the scale factor and unit cell parameters were the only variables.

(5) The parameters U, V, and W in the equation (*4*)

$$H^2 = U \tan^2\theta + V \tan\theta + W$$

(where H is the full width at half height of the Gaussian curve for the reflection at Bragg angle θ) were determined from a least-squares fit, to the above equation, of the measured half height widths of five reflections in the diffraction pattern of annealed nickel powder (all the reflections in the face-centered cubic pattern up to the 222 reflection were used).

(6) The θ zero point and asymmetry parameters were both set initially to zero.

The neutron scattering amplitudes used were $b_{Ce} = 4.8$ fm (*7*); $b_{Nd} = 7.69$ fm (*8*); $b_c = 6.65$ fm (*7*). In the mixed cerium/neodymium compositions, the effective metal-atom scattering amplitudes were the appropriately weighted means of those for cerium and neodymium.

On the VANESSA diffractometer, there is an increase in background count at high Bragg angles. This arises from the main beam neutrons and is due to the limitations of the shielding which are imposed by the vertical arrangement of the diffractometer. Because of uncertainty in the background counts at high angles in the powder patterns, refinement was limited to the low-angle region $2\theta = 10°$ to $2\theta = 60°$.

The tendency for nonpositive definite thermal parameters in the least-squares minimizations was overcome by applying a small fraction (in some cases only one-hundredth) of the calculated shift to each of the thermal parameters, and by extending refinement to 20–30 cycles. In the final cycle of all five refinements, the shift in any parameter did not exceed one-quarter of the estimated standard deviation (ESD) and in most cases was very much smaller. Correlation matrices from the final cycles of refinement indicated significant correlations between shifts for parameters within the following groups:

(1) Anisotropic thermal parameters (coefficients up to 0.6); (2) U, V, and W (coefficients greater than 0.9); and (3) Unit cell, zero point, and asymmetry parameters (coefficients from 0.5 to 0.9).

Shifts in the scale factor showed correlations (with coefficients up to 0.7) with some of the thermal parameter shifts. The z parameter of the carbon atom was not strongly correlated with any other parameter (maximum coefficient = 0.2). Figure 1 illustrates the observed, calculated, and discrepancy profiles for one of the compounds. Lists of observed and calculated intensities for all points for the five structures have been deposited.[1]

Application of absorption corrections (coefficients μ in Table I calculated from mass absorption coefficients Ce, 0.0021; Nd, 0.11; C, 0.00015 $cm^2\ g^{-1}$) in accordance with the Hewat procedure (*9*) produces corrections, ΔB, to the thermal parameters (Table I) which are smaller than the apparent ESDs. Although anisotropic refinement indicated that Ce undergoes greater thermal motion in the x and y than in the z direction (contrast the $Y_xHo_{1-x}C_2$ series (*5*)), we list

---

[1] See NAPS document No. 04350 for 5 pages of supplementary material. Order from ASIS/NAPS, Microfiche Publications, P.O. Box 3513, Grand Central Station, New York, N.Y. 10163. Remit in advance $4.00 for microfiche copy or for photocopy, $7.75 up to 20 pages plus $0.30 for each additional page. All orders must be prepaid. Institutions and organizations may order by purchase order. However, there is a billing and handling charge for this service of $15. Foreign orders add $4.50 for postage and handling, for the first 20 pages, and $1.00 for additional 10 pages of material. Remit $1.50 for postage of any microfiche orders.

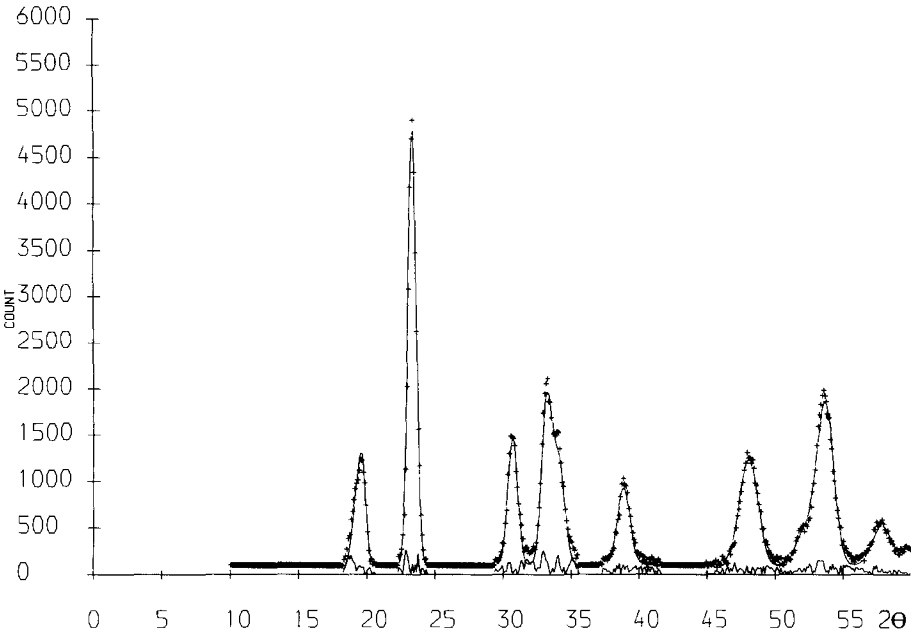

FIG. 1. Neutron powder diffraction diagram for $Ce_{0.25}Nd_{0.75}C_2$: solid line, calculated profile; crosses, experimental intensities; differences between these are shown at the bottom.

only equivalent isotropic parameters (*10*) in Table I in view of high ESDs.

3. Results and Discussion

Throughout the composition range, a tetragonal structure predominates; Table I shows the final refined structural parameters for the five dicarbides. Overall, the R values (Table I, defined as in (*5*)) and ESDs in this series are higher than for the $Y_xHo_{1-x}C_2$ series, as expected from the lower quality of the data.

As cerium content decreases, both the unit cell dimensions decrease progressively. For the a and c dimensions of CeC_2 and NdC_2, the earlier X-ray data (*2*) are in good agreement with the new profile-refined results, indeed better than are the earlier neutron data (*3*).

The C–C bond lengths pass through a minimum in the middle of the composition range, presumably indicative of rather stronger bonding at this composition. A similar but smaller effect, not statistically significant, was noted in the yttrium–holmium ternary dicarbides (*5*). While the C–C bond length of 1.297(5) Å in CeC_2 may possibly be significantly longer than the

TABLE I

RESULTS OF NEUTRON POWDER PROFILE REFINEMENTS FOR FIVE $Ce_xNd_{1-x}C_2$ COMPOUNDS

x	1	0.75	0.50	0.25	0
a	3.881(2)	3.872(2)	3.850(2)	3.843(2)	3.827(2)
c	6.487(3)	6.476(3)	6.440(3)	6.432(3)	6.407(2)
z_c	0.4000(4)	0.4006(4)	0.4010(4)	0.3999(5)	0.3984(4)
B(M)	0.87(0.32)	1.06(0.33)	0.67(0.33)	0.33(0.37)	0.48(0.36)
B(C)	0.73(0.16)	0.67(0.19)	0.66(0.24)	0.61(0.30)	0.47(0.33)
μ	0.01	0.14	0.28	0.42	0.56
ΔB	0.0001	0.002	0.005	0.01	0.02
R	0.097	0.106	0.112	0.114	0.107
R_w	0.111	0.117	0.119	0.123	0.115
C–C (Å)	1.297(5)	1.287(5)	1.275(5)	1.288(6)	1.302(5)
M–C (Å)	2.595(3)	2.594(3)	2.582(3)	2.572(3)	2.553(3)

Note. Unit cell dimensions a and c (Å), fractional z coordinates of carbon z_c, equivalent isotropic temperature factors B^2 ($Å^2$), absorption coefficients μ (cm^{-1}), absorption corrections ΔB to B, unweighted (R), and weighted (R_w) agreement factors, and C–C and mean metal–C bond lengths (Å) (ESDs of least significant figures in parentheses). R and R_w are as defined previously (*5*).

value of 1.281(7) Å found by Atoji (*3*) at 5 K, the length in NdC_2 is not significantly different from that found by Atoji. As Nd content increases, the average metal–carbon bond length shortens from 2.595(3) Å in CeC_2 to 2.553(3) Å in NdC_2 (Table I).

Finally, we note that the refined values for the three half height width parameters, the zero point parameters, and asymmetry parameters do not differ significantly throughout the five structures.

Acknowledgments

We are grateful to the SRC/SERC for access to neutron beam facilities and for financial support to J.Y.

References

1. I. J. McColm, T. A. Quigley, and N. J. Clark, *J. Inorg. Nucl. Chem.* **35,** 1931 (1973).
2. F. H. Spedding, K. G. Schneider, and A. H. Daane, *J. Amer. Chem. Soc.* **80,** 4499 (1958).
3. M. Atoji, *J. Chem. Phys.* **46,** 1891 (1967).
4. H. M. Rietveld, *J. Appl. Crystallogr.* **2,** 65 (1969).
5. D. W. Jones, I. J. McColm, R. Steadman, and J. Yerkess, *J. Solid-State Chem.* **53,** 376 (1984).
6. W. J. A. M. Peterse and J. H. Palm, *Acta Crystallogr.* **20,** 147 (1966).
7. G. E. Bacon, *Acta Crystallogr. A* **28,** 357 (1972).
8. J. X. Boucherle, *Acta Crysallogr. B* **31,** 2745 (1975).
9. A. W. Hewat, *Acta Crystallogr. A* **35,** 248 (1979).
10. W. C. Hamilton, *Acta Crystallogr.* **12,** 609 (1959).